PHYSICAL REVIEW A **89**, 061603(R) (2014)

Floquet topological states in shaking optical lattices

Wei Zheng and Hui Zhai
Institute for Advanced Study, Tsinghua University, Beijing 100084, China
(Received 24 February 2014; revised manuscript received 11 March 2014; published 27 June 2014)

In this Rapid Communication we propose realistic schemes to realize topologically nontrivial Floquet states by shaking optical lattices, using both the one-dimensional lattice and two-dimensional honeycomb lattice as examples. The topological phase in the two-dimensional model exhibits quantum anomalous Hall effect. The transition between topological trivial and nontrivial states can be easily controlled by both shaking frequency and shaking amplitude. Our schemes have two major advantages. First, both the static Hamiltonian and the shaking scheme are sufficiently simple to implement. Secondly, it requires relatively small shaking amplitude and therefore heating can be minimized. These two advantages make our schemes much more practical.

DOI: 10.1103/PhysRevA.89.061603 PACS number(s): 67.85.−d, 03.75.Ss

Introduction. Topological states of matter have been extensively studied in equilibrium systems. Recently, topological nontrivial quantum states have been proposed in a periodically driven nonequilibrium system called "Floquet topological insulators" [1–3]. The Floquet topological band has been first realized in photonic crystals and the edge state of light has been observed [4], while so far it has not been realized in any solid-state or cold-atom system.

Realizing and studying the topological state of matter is also one of the major trends for cold atom physics nowadays, for which Raman laser coupling [5–12] and shaking optical lattice [13–15] have been developed. It has been demonstrated that fast shaking optical lattices can generate synthetic Abelian gauge field and magnetic flux [13,14], and various theoretical proposals also exist [16–25]. In this Rapid Communication we propose that shaking optical lattice is also a powerful tool to realize Floquet topological states in cold-atom systems. We demonstrate that a system equivalent to the Su-Schrieffer-Heeger model in one dimension [26] and a system equivalent to the Haldane model [28] in a two-dimensional honeycomb lattice [27] can be realized, and the latter exhibits quantum anomalous Hall effect.

So far, quantum anomalous Hall effect has only been found in chromium-doped $(Bi,Sb)_2Te_3$, and growing this material is extremely challenging [29]. It is therefore highly desirable that one can quantum simulate this effect with the cold-atom system. However, although there already exist several proposals using atom-light interactions [20–25], this effect has not yet been realized in a cold-atom setup. The key technique challenge is to have a scheme that is sufficiently simple to be implemented within a currently available experimental setup and can also avoid unwanted heating. Our scheme fulfills these two requirements and therefore can help to overcome this challenge.

The first is its simplicity. To realize a topological state in a static system, it usually requires a particular form of hopping term. For instance, in order to realize the Haldane model [28], one needs to generate a special next-nearest range hopping term, which usually requires engineering laser-assisted tunneling in a cold-atom system [9–12]. In contrast, in our scheme, the static Hamiltonian is quite simple (it only contains normal nearest neighboring hopping without an extra phase factor) and has been realized in different laboratories already. We will show that the beauty of this scheme is that such a simple static Hamiltonian can result in a topological nontrivial state when a proper and also sufficiently simple way of shaking is turned on.

The second is minimizing heating. In contrast to other shaking schemes [13,14], a key ingredient of our scheme is that shaking provides a resonant coupling between different bands; therefore, as we shall show later, it only demands a shaking amplitude much smaller than lattice spacing in order to reach the topological phase, and consequently this scheme avoids the heating problem often encountered in schemes utilizing atom-light interactions. In a recent experiment by a Chicago group, it is found that heating from such a small shaking amplitude is insignificant [15].

We also remark that our shaking scheme in a honeycomb lattice can be regarded mathematically as generating a synthetic circular polarized light for neutral atoms [1,30]. However, to realize this with real light in graphene the required frequency has to be in a soft x-ray regime [30] which makes the experiment extremely challenging. While in our scheme the required shaking frequency is within a very practical regime of about hundreds of hertz.

General method. Our theoretical treatment of shaking optical lattices is based on the Floquet theory. The Floquet operator of a periodically driven Hamiltonian $\hat{H}(t)$ with period T is defined as ($\hbar = 1$)

$$\hat{F} = \hat{U}(T_i + T, T_i) = \hat{\mathcal{T}} \exp\left\{-i \int_{T_i}^{T_i+T} dt\, \hat{H}(t)\right\}, \quad (1)$$

where $\hat{\mathcal{T}}$ denotes time order, and T_i is the initial time. The eigenvalue and eigenstates of $\hat{F}$ are given by

$$\hat{F}|\varphi_n\rangle = e^{-i\varepsilon_n T}|\varphi_n\rangle, \quad (2)$$

where $-\pi/T < \varepsilon_n < \pi/T$ is the quasienergy. Below, two different methods are used to evaluate the Floquet operator, and each method has its own advantage.

Method I. We can numerically evaluate Floquet operator $\hat{F}$ according to Eq. (1) and determine its eigenvalues and eigen-wave-functions from Eq. (2). If a periodically driven system exhibits nontrivial topological states, there must be in-gap quasienergies ϵ and their corresponding wave functions φ are spatially well localized at the edge of the system [2]. The advantage of this method is that once $\hat{H}(t)$ is given, there are no further approximations.

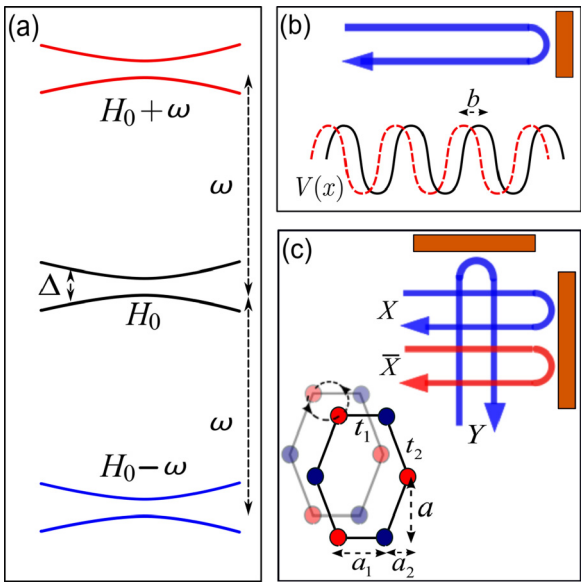

FIG. 1. (Color online) (a) The typical energy structure under consideration. (b) The laser setup of the one-dimensional shaking optical lattice. Solid and dashed lines represent lattice potential at two different times. (c) The laser setup of the two-dimensional honeycomb optical lattice. The dashed circle with arrow indicates how each lattice potential rotates in time.

Method II. We can introduce a time-independent effective Hamiltonian $\hat{H}_{\rm eff}$ via $\hat{F} = e^{-i\hat{H}_{\rm eff}T}$. Expanding $\hat{H}(t)$ as $\hat{H}(t) = \sum_{n=-\infty}^{\infty} \hat{H}_n(t) e^{in\omega t}$ with $\omega = 2\pi/T$, we consider a situation as shown in Fig. 1(a), that is, the static component $\hat{H}_0$ contains m bands within an energy range of Δ and $\omega \gg \Delta$. The two concrete examples discussed below either belong to this situation or can be transferred into this situation by a rotating wave transformation, with $m = 2$. Under this condition, it is straightforward to show that to the leading order of Δ/ω, $\hat{H}_{\rm eff}$ can be deduced as

$$\hat{H}_{\rm eff} = \hat{H}_0 + \sum_{n=1}^{\infty} \left\{ \frac{[\hat{H}_n, \hat{H}_{-n}]}{n\omega} - \frac{[\hat{H}_n, \hat{H}_0]}{e^{-2\pi n i\alpha} n\omega} + \frac{[\hat{H}_{-n}, \hat{H}_0]}{e^{2\pi n i\alpha} n\omega} \right\}, \tag{3}$$

where T_i is taken as αT with $0 \leqslant \alpha < 1$. Since $\hat{F}$ with different choices of initial time T_i relate to each other by a unitary transformation, quasienergy is independent of the choice of T_i. In particular, we can choose an optimal α that simplifies $\hat{H}_{\rm eff}$. Then we can apply schemes developed for a time-independent Hamiltonian to $\hat{H}_{\rm eff}$ for classifying the topology of this time-periodic system. Although this method involves further approximations, it has the advantage that it is physically more transparent and can bring out the connection to topological phenomena in equilibrium systems.

One-dimensional case. A one-dimensional lattice is formed by two counterpropagating lasers. As one time-periodically modulates the relative phase θ between two lasers, it will result in a time-dependent lattice potential [31,32], as shown in Fig. 1(b),

$$H(t) = \frac{\hat{k}_x^2}{2m} + V \cos^2[k_r x + \theta(t)], \tag{4}$$

where $\theta(t) = k_r b \cos(\omega t)$, and b is the maximum lattice displacement. By transferring to the comoving frame, $x \to x + b\cos(\omega t)$, the Hamiltonian acquires a time-dependent vector potential term as

$$H(t) = \frac{\hat{k}_x^2}{2m} + V \cos^2(k_r x) - b\omega \sin(\omega t) \cdot \hat{k}_x. \tag{5}$$

The first two static terms give a static band structure with Bloch wave function $\varphi_\lambda(k_x)$. In this basis, by only keeping the s and p bands, we can write down a tight-binding Hamiltonian as

$$\hat{H}(t) = \sum_i \hat{\Psi}_i^\dagger K(t) \hat{\Psi}_i + \sum_i [\hat{\Psi}_i^\dagger J(t) \hat{\Psi}_{i+1} + \text{H.c.}], \tag{6}$$

where $\hat{\Psi}_i^\dagger = (\hat{a}_{p,i}^\dagger, \hat{a}_{s,i}^\dagger)$ are creation operators for s and p orbitals, and

$$K(t) = \begin{pmatrix} \epsilon_p & ih_0^{sp}\sin(\omega t) \\ -ih_0^{sp}\sin(\omega t) & \epsilon_s \end{pmatrix}, \tag{7}$$

$$J(t) = \begin{pmatrix} t_p - ih_1^{pp}\sin(\omega t) & ih_1^{sp}\sin(\omega t) \\ -ih_1^{sp}\sin(\omega t) & t_s - ih_1^{ss}\sin(\omega t) \end{pmatrix}, \tag{8}$$

where ϵ_s and ϵ_p are the on-site energy, t_s and t_p are the hopping amplitude from the static part, and $h_0^{sp} = b\omega \int dx\, \phi_s(x)\, \partial_x \phi_p(x)$ denotes shaking-induced on-site coupling processes. $h_1^{\lambda\lambda'} = b\omega \int dx\, \phi_\lambda(x-a)\, \partial_x \phi_{\lambda'}(x)$, where $\lambda\lambda' = ss, pp, sp$ denotes shaking-induced nearest neighboring hopping processes. Here $\phi_s(x)$ and $\phi_p(x)$ are the Wannier wave functions of the s orbit and the p orbit, and $a = \pi/k_r$ is the lattice constant. For a given lattice depth V, ϵ_s, ϵ_p, t_s, and t_p are fixed, and h_0^{sp}, h_1^{ss}, h_1^{pp}, and h_1^{sp} scale linearly with $k_r b$.

With the Hamiltonian equations (6)–(8) and method I, we find phase transitions between topological trivial and nontrivial phases, by changing frequency via $\Delta_0 = (\epsilon_p - \epsilon_s - 2\omega)/2$ and shaking amplitude $k_r b$. A phase diagram is shown in Fig. 2(a). The topological nontrivial state possesses a pair

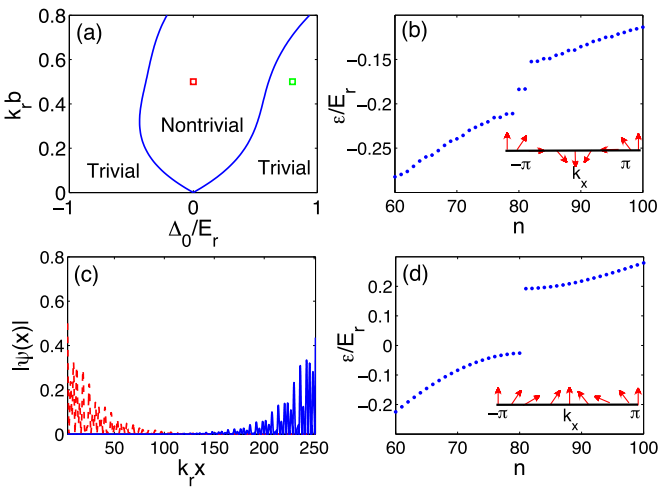

FIG. 2. (Color online) (a) Phase diagram in terms of shaking frequency Δ_0/E_r and shaking amplitude $k_r b$. $V = 3E_r$ is fixed. (b), (d) Quasienergy spectrum of a finite size one-dimensional shaking optical lattice. $\Delta_0/E_r = 0$ and $k_r b = 0.5$ for (b); and $\Delta_0/E_r = 0.8$ and $k_r b = 0.5$ for (d), as marked in (a). Inset: Winding of $\mathbf{B}(k_x)$ in the yz plane as k_x changes from $-\pi$ to π. See text for a definition of $\mathbf{B}(k_x)$. (c) The wave functions for the in-gap states of (b).

of in-gap states in the quasienergy spectrum of a finite size lattice, as shown in Fig. 2(b), whose corresponding wave functions are well localized in the edges [see Fig. 2(c)]. In contrast, in the topological trivial regime, there is no in-gap state in the quasienergy spectrum [see Fig. 2(d)]. As one can see clearly in Fig. 2(d), even for a relatively small shaking amplitude $k_r b \approx 0.1$, there is a quite large regime for topological nontrivial phase in the phase diagram.

To understand the emergence of the topological nontrivial phase, we write the Hamiltonian into momentum space as $\hat{H}(t) = \sum_{k_x} \hat{\Psi}^\dagger_{k_x} H_{k_x} \hat{\Psi}_{k_x}$ (k_x in units of $1/a$, where a is lattice spacing) and H_{k_x} is given by

$$H_{k_x} = \begin{pmatrix} \epsilon_p + 2t_p \cos\, k_x & 0 \\ 0 & \epsilon_s + 2t_s \cos\, k_x \end{pmatrix} + \sin(\omega t) \times \begin{pmatrix} 2h_1^{pp} \sin\, k_x & i\left(h_0^{sp} + 2h_1^{sp} \cos\, k_x\right) \\ -i\left(h_0^{sp} + 2h_1^{sp} \cos\, k_x\right) & 2h_1^{ss} \sin\, k_x \end{pmatrix}. \tag{9}$$

With two-phonon resonance condition $2\omega \approx \epsilon_p - \epsilon_s$, the p band with dispersion $\epsilon_p + 2t_p \cos(k_x)$ and the two-phonon dressed s band with dispersion $\epsilon_s + 2\omega + 2t_s \cos(k_x)$ form two close bands as schematized in Fig. 1(a). Therefore, we shall first apply a unitary rotation $O(t) = \exp(i\omega t \sigma_z)$ that leads to

$$\hat{H}_{\rm rot}(t) = \hat{H}_0 + \sum_{n=\pm1,\pm3} \hat{H}_n e^{in\omega t}. \tag{10}$$

Here $\hat{H}_0 = (\Delta_0 + 2t \cos\, k_x)\sigma_z$, $\hat{H}_1 = -ih_1 \sin\, k_x \sigma_z - (h_0^{sp} + 2h_1^{sp} \cos k_x)\sigma_+/2$, $\hat{H}_3 = (h_0^{sp} + 2h_1^{sp} \cos\, k_x)\sigma_+/2$, and $\hat{H}_{-n} = \hat{H}_n^\dagger$, where $2t = t_p - t_s$, $2h_1 = h_1^{pp} - h_1^{ss}$. In the tight-binding regime, we have $\omega \gg \Delta_0, t, h_0^{sp}, h_1^{\lambda\lambda}$. Thus, it fulfills the condition to apply method II. By choosing $T_i = T/4$ and following the formula, Eq. (3), the effective Hamiltonian can be deduced as $H_{\rm eff} = \mathbf{B}(k_x) \cdot \sigma$, where $B_x = 0$ and

$$B_y = \frac{2\left(h_0^{sp} + 2h_1^{sp} \cos\, k_x\right)}{\omega}\left[h_1 \sin\, k_x - \frac{2(\Delta_0 + 2t\, \cos\, k_x)}{3}\right],$$

$$B_z = \Delta_0 + 2t\, \cos\, k_x + \frac{2\left(h_0^{sp} + 2h_1^{sp} \cos\, k_x\right)^2}{3\omega}. \tag{11}$$

This describes a momentum-dependent magnetic field in the yz plane of the Bloch sphere, which is analogous to momentum space representation of the Su-Schrieffer-Heeger model [26]. The Su-Schrieffer-Heeger model exhibits topological nontrivial phases characterized by a nonzero Zak phase [33], which has been realized and measured recently in double-well optical lattices [34]. Whether the system is topologically trivial or not depends on whether $\mathbf{B}(k_x)$ has a nonzero winding number in the yz plane as k_x changes from $-\pi$ to π. As shown in the inset of Figs. 2(b) and 2(d), for the topological trivial case of Fig. 2(b), $\mathbf{B}(k_x)$ has a winding number zero; while for the topological nontrivial case of Fig. 2(b), the winding number of $\mathbf{B}(k_x)$ equals 1. From Eq. (11), it is easy to see that when $|\Delta_0|$ is large enough, B_z is dominated by the constant term and therefore $\mathbf{B}(k_x)$ has no winding. That explains why the topological nontrivial phase occurs around the two-phonon resonance regime with $\Delta_0 \approx 0$. In fact, the two-phonon resonance condition plays a crucial role here. In contrast, if we consider the one-phonon resonance regime $\omega \sim \epsilon_p - \epsilon_s$, with similar analysis it is straightforward to show that there will be no topological nontrivial phase [35].

Two-dimensional case. We employ the laser setup for a two-dimensional honeycomb lattice used by the ETH group [27], as shown in Fig. 1(c). The interference of X and Y beams gives a checkerboard of spacing $\lambda/\sqrt{2}$. $\bar{X}$ gives an additional standing wave with spacing $\lambda/2$. When $V_{\bar{X}} \gg V_Y \gtrsim V_X$, it leads to a honeycomb lattice as shown in Fig. 1(c). Using the same method as in the one-dimensional case, the optical lattice can be shaken in both x and y directions with a phase difference $\pi/2$. This gives rise to a time-dependent potential:

$$\begin{aligned} V(x,y,t) &= -V_{\bar{X}} \cos^2[k_r(x + b\, \cos\, \omega t) + \theta/2] \\ &\quad - V_X \cos^2[k_r(x + b \cos \omega t)] - V_Y \cos^2[k_r(y + b \sin \omega t)] \\ &\quad -2\alpha\sqrt{V_X V_Y}[\cos k_r(x + b \cos \omega t)] \cos[k_r(y + b \sin \omega t)]. \end{aligned}$$

Here θ controls the energy offset M between the AB sublattices of a honeycomb lattice. Similarly, by transferring into the comoving frame $x \to x + b \cos(\omega t)$, and $y \to y + b \sin(\omega t)$, one obtains a Hamiltonian with time-dependent vector potential term

$$H(t) = \frac{1}{2m}[\mathbf{k} - \mathbf{A}(t)]^2 + V(x,y), \tag{12}$$

where $A_x(t) = m\omega b \sin(\omega t)$ and $A_y(t) = -m\omega b \cos(\omega t)$. It is equivalent to an ac electrical field in the two-dimensional plane $\mathbf{E}(t) = m\omega^2 b(\cos(\omega t), \sin(\omega t))$ [30]. With the tight-binding approximation and Peierls substitution, the Hamiltonian is given by

$$\hat{H}(t) = \sum_{\langle ij \rangle} (a^\dagger_{A,j}, a^\dagger_{B,j}) \begin{pmatrix} M\delta_{ji} & t_l e^{i\mathbf{A}(t)\cdot\mathbf{d}_{ji}} \\ \text{H.c.} & -M\delta_{ji} \end{pmatrix} \begin{pmatrix} a_{A,i} \\ a_{B,i} \end{pmatrix}, \tag{13}$$

where $\mathbf{d}_{ji}$ is the vector from site i pointing to site j, and t_l is the hopping amplitude schematically shown in Fig. 1(c).

Applying method I to this model, we find a similar phase diagram that contains topological trivial and nontrivial phases, as shown in Fig. 3(a). In this case, the phase diagram is controlled by parameter M/E_r and shaking amplitude $k_r b$. Similarly, the topological trivial phase has no in-gap states in the quasienergy spectrum [Fig. 3(d)], and the topological nontrivial phase has a pair of in-gap states [Fig. 3(b)], whose corresponding wave function [Fig. 3(c)] is localized at the edge of the two-dimensional sample. The same as the one-dimensional case, even for a small shaking amplitude of $k_r b \approx 0.1$, the topological nontrivial regime occupies a large parameter space.

To illustrate the relation of this topological nontrivial phase with the Haldane model and the quantum anomalous Hall effect, we first expand Hamiltonian equation (13) as $H(\mathbf{k},t) = \sum_{n=-\infty}^{\infty} \hat{H}_n(\mathbf{k}) e^{in\omega t}$. $\hat{H}_0$ gives rise to a static honeycomb lattice structure, which contains two bands with bandwidth $\sim 2t_l$ and band gap $\sim 2M$. When $\omega \gg 2M, 2t_l$, the condition for applying Method II is satisfied, and it yields an effective Hamiltonian $H_{\rm eff}(\mathbf{k}) = \mathbf{B}(\mathbf{k}) \cdot \sigma$. The explicit form of $\mathbf{B}(\mathbf{k})$

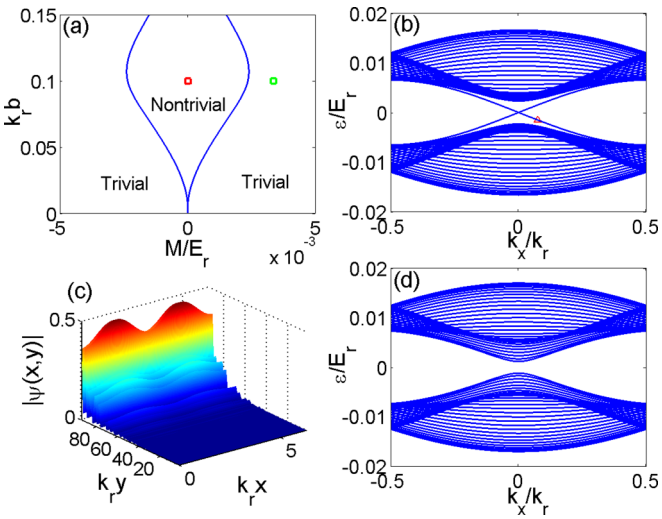

FIG. 3. (Color online) (a) Phase diagram in terms of the on-site energy difference of the AB sublattice of a honeycomb lattice M/E_r and the shaking amplitude $k_r b$. ω/E_r is fixed at 0.2. (b), (d) Quasienergy spectrum of a finite size two-dimensional shaking honeycomb lattice with armchair edge. $M/E_r = 0$ and $k_r b = 0.1$ for (b) and $M/E_r = 0.003$ and $k_r b = 0.1$ for (d), as marked in (a). (c) The wave functions for the in-gap states of (b). The lattice potential $V_{\bar{X}}/E_r = 5$, $V_X/E_r = 0.65$, $V_Y/E_r = 2$, and $\alpha = 0.8$.

is given in the Supplemental Material [35]. This effective Hamiltonian can be compared with the Haldane model. If $\mathbf{B}(\mathbf{k})$ fully covers the Bloch sphere as $\mathbf{k}$ goes over the Brillouin zone, this phase is topologically nontrivial and exhibits quantum anomalous Hall effect [28].

For small shaking amplitude, at the leading order of $k_r b$, $B_x(\mathbf{k})$ and $B_y(\mathbf{k})$ are given by the static part of the honeycomb lattice Hamiltonian. Due to the Dirac point structure, $\{B_x, B_y\}$ has desired winding structure in the xy plane. $B_z(\mathbf{k})$ can be generally written as $M + D(\mathbf{k})$, where $D(\mathbf{k})$ represents terms generated by shaking, and therefore for small shaking amplitude, $D(\mathbf{k})$ scales linearly with $k_r b$. If $|M| > D(\mathbf{k})$ for all $\mathbf{k}$, either due to small $k_r b$ or large $|M|$, B_z always has the same sign as M and therefore spin can only point to half of the Bloch sphere; the resulting state will still be topological trivial, as shown in Fig. 3(d).

As $k_r b$ increases, $D(\mathbf{k})$ will become larger than M in a certain regime of $\mathbf{k}$ space. In particular, for our model, similar to the case of the Haldane mode, $D(\mathbf{k})$ takes opposite sign between two Dirac points (where both B_x and B_y vanish), and its absolute value is larger than $|M|$. Thus, B_z takes opposite values between two Dirac points and the spin vector points to north and south poles, respectively, at two Dirac points. This feature, together with nontrivial winding of $\{B_x, B_y\}$ in the xy plane, gives rise to a topologically nontrivial coverage of spin vector in the Bloch sphere. Consequently, it enters topological nontrivial phase, with a nonzero Chern number and chiral edge state, as shown in Fig. 3. With noninteracting fermions in this setup, it will exhibit quantum anomalous Hall effect with quantized Hall conductance, which can be measured by various methods [20,36–38].

We believe the schemes and examples presented in this work open a route toward realizing topological states in cold-atom systems. It will be very interesting to generalize the current work to three dimensions and the case with interactions.

Acknowledgments. We wish to thank Cheng Chin for many simulating discussions. This work is supported by Tsinghua University Initiative Scientific Research Program, NSFC Grant No. 11174176, and NKBRSFC under Grant No. 2011CB921500.

[1] T. Oka and H. Aoki, Phys. Rev. B **79**, 081406(R) (2009).
[2] T. Kitagawa, E. Berg, M. Rudner, and E. Demler, Phys. Rev. B **82**, 235114 (2010).
[3] N. H. Lindner, G. Refael, and V. Galitski, Nat. Phys. **7**, 490 (2011).
[4] M. C. Rechtsman, J. M. Zeuner, Y. Plotnik, Y. Lumer, D. Podolsky, F. Dreisow, S. Nolte, M. Segev, and A. Szameit, Nature (London) **496**, 196 (2013).
[5] Y.-J. Lin, R. L. Compton, K. Jiménez-García, J. V. Porto, and I. B. Spielman, Nature (London) **462**, 628 (2009).
[6] Y.-J. Lin, K. Jiménez-García, and I. B. Spielman, Nature (London) **471**, 83 (2011).
[7] P.-J. Wang, Z.-Q. Yu, Z. Fu, J. Miao, L. Huang, S. Chai, H. Zhai, and J. Zhang, Phys. Rev. Lett. **109**, 095301 (2012).
[8] L. W. Cheuk, A. T. Sommer, Z. Hadzibabic, T. Yefsah, W. S. Bakr, and M. W. Zwierlein, Phys. Rev. Lett. **109**, 095302 (2012).
[9] M. Aidelsburger, M. Atala, S. Nascimbène, S. Trotzky, Y.-A. Chen, and I. Bloch, Phys. Rev. Lett. **107**, 255301 (2011).
[10] K. Jiménez-García, L. J. LeBlanc, R. A. Williams, M. C. Beeler, A. R. Perry, and I. B. Spielman, Phys. Rev. Lett. **108**, 225303 (2012).
[11] M. Aidelsburger, M. Atala, M. Lohse, J. T. Barreiro, B. Paredes, and I. Bloch, Phys. Rev. Lett. **111**, 185301 (2013).
[12] H. Miyake, G. A. Siviloglou, C. J. Kennedy, W. Cody Burton, and W. Ketterle, Phys. Rev. Lett. **111**, 185302 (2013).
[13] J. Struck, C. Ölschläger, R. Le Targat, P. Soltan-Panahi, A. Eckardt, M. Lewenstein, P. Windpassinger, and K. Sengstock, Science **333**, 996 (2011).
[14] J. Struck, C. Ölschläger, M. Weinberg, P. Hauke, J. Simonet, A. Eckardt, M. Lewenstein, K. Sengstock, and P. Windpassinger, Phys. Rev. Lett. **108**, 225304 (2012).
[15] C. V. Parker, L. C. Ha, and C. Chin, Nat. Phys. **9**, 769 (2013).
[16] A. S. Sørensen, E. Demler, and M. D. Lukin, Phys. Rev. Lett. **94**, 086803 (2005).
[17] N. R. Cooper, Phys. Rev. Lett. **106**, 175301 (2011).
[18] K. Sun, W. Vincent Liu, A. Hemmerich, and S. Das Sarma, Nat. Phys. **8**, 67 (2012).
[19] P. Hauke, O. Tieleman, A. Celi, C. Ölschläger, J. Simonet, J. Struck, M. Weinberg, P. Windpassinger, K. Sengstock, M. Lewenstein, and A. Eckardt, Phys. Rev. Lett. **109**, 145301 (2012).
[20] L. B. Shao, Shi-Liang Zhu, L. Sheng, D. Y. Xing, and Z. D. Wang, Phys. Rev. Lett. **101**, 246810 (2008).

[21] N. Goldman, A. Kubasiak, A. Bermudez, P. Gaspard, M. Lewenstein, and M. A. Martin-Delgado, Phys. Rev. Lett. **103**, 035301 (2009).

[22] X. J. Liu, X. Liu, C. Wu, and J. Sinova, Phys. Rev. A **81**, 033622 (2010).

[23] M. Zhang, H. H. Hung, C. Zhang, and C. Wu, Phys. Rev. A **83**, 023615 (2011).

[24] E. Alba, X. Fernandez-Gonzalvo, J. Mur-Petit, J. K. Pachos, and J. J. Garcia-Ripoll, Phys. Rev. Lett. **107**, 235301 (2011).

[25] N. Goldman, E. Anisimovas, F. Gerbier, P. Öhberg, I. B. Spielman and G. Juzeliunas, New J. Phys. **15**, 013025 (2013).

[26] W. P. Su, J. R. Schrieffer, and A. J. Heeger, Phys. Rev. Lett. **42**, 1698 (1979).

[27] L. Tarruell, D. Greif, T. Uehlinger, G. Jotzu, and T. Esslinger, Nature (London) **483**, 302 (2012).

[28] F. D. M. Haldane, Phys. Rev. Lett. **61**, 2015 (1988).

[29] C.-Z. Chang, J. Zhang, X. Feng, J. Shen, Z. Zhang, M. Guo, K. Li, Y. Ou, P. Wei, L.-L. Wang, Z.-Q. Ji, Y. Feng, S. Ji, X. Chen, J. Jia, X. Dai, Z. Fang, S.-C. Zhang, K. He, Y. Wang, L. Lu, X.-C. Ma, and Q.-K. Xue, Science **340**, 167 (2013).

[30] The system of circularly polarized light on graphene has been studied by Ref. [1] and T. Kitagawa, T. Oka, A. Brataas, L. Fu, and E. Demler, Phys. Rev. B **84**, 235108 (2011).

[31] N. Gemelke, E. Sarajlic, Y. Bidel, S. Hong, and S. Chu, Phys. Rev. Lett. **95**, 170404 (2005).

[32] H. Lignier, C. Sias, D. Ciampini, Y. Singh, A. Zenesini, O. Morsch, and E. Arimondo, Phys. Rev. Lett. **99**, 220403 (2007).

[33] J. Zak, Phys. Rev. Lett. **62**, 2747 (1989).

[34] M. Atala, M. Aidelsuburger, J. T. Barreiro, D. Abanin, T. Kitagawa, E. Demler, and I. Blcoh, Nat. Phys. **9**, 795 (2013).

[35] See Supplemental Material at http://link.aps.org/supplemental/10.1103/PhysRevA.89.061603 for (i) one-phonon transition regime of the one-dimensional optical lattice case and (ii) the explicit definition for $\mathbf{B}(\mathbf{k})$ for the two-dimensional honeycomb model.

[36] R. O. Umucalilar, H. Zhai, and M. Ö. Oktel, Phys. Rev. Lett. **100**, 070402 (2008).

[37] E. Zhao, N. Bray-Ali, C. J. Williams, I. B. Spielman, and I. I. Satija, Phys. Rev. A **84**, 063629 (2011).

[38] N. Goldman, J. Beugnon, and F. Gerbier, Phys. Rev. Lett. **108**, 255303 (2012).